Interictal Electrophysiological Source Imaging Based on Realistic Epilepsy Head Model in Presurgical Evaluation: A Prospective Study*

Ruowei Qu[1], *Zhaonan Wang*[1], *Shifeng Wang*[2], *Le Wang*[3], *Alan Wang*[4] *and Guizhi Xu*[1*]
(1. State Key Laboratory of Reliability and Intelligence of Electrical Equipment, Hebei University of Technology, Tianjin 300401, China;
2. Tianjin Universal Medical Imaging Diagnostic Center, Tianjin 300110, China;
3. Department of Functional Neurosurgery, Huanhu Hospital, Tianjin 300350, China;
4. Auckland Bioengineering Institute, The University of Auckland, Grafton, Auckland 1010, New Zealand)

Abstract: Invasive techniques are becoming increasingly important in the presurgical evaluation of epilepsy. Adopting the electrophysiological source imaging (ESI) of interictal scalp electroencephalography (EEG) to localize the epileptogenic zone remains a challenge. The accuracy of the preoperative localization of the epileptogenic zone is key to curing epilepsy. The T1 MRI and the boundary element method were used to build the realistic head model. To solve the inverse problem, the distributed inverse solution and equivalent current dipole (ECD) methods were employed to locate the epileptogenic zone. Furthermore, a combination of inverse solution algorithms and Granger causality connectivity measures was evaluated. The ECD method exhibited excellent focalization in lateralization and localization, achieving a coincidence rate of 99.02% (p<0.05) with the stereo electroencephalogram. The combination of ECD and the directed transfer function led to excellent matching between the information flow obtained from intracranial and scalp EEG recordings. The ECD inverse solution method showed the highest performance and could extract the discharge information at the cortex level from noninvasive low-density EEG data. Thus, the accurate preoperative localization of the epileptogenic zone could reduce the number of intracranial electrode implantations required.

Keywords: Epilepsy, epileptogenic zone, realistic head model, functional brain connectivity, ESI

1 Introduction

Epilepsy, defined as a sudden and recurring brain dysfunction, has surpassed most common neurological diseases, and is second only to headaches. According to the latest epidemiological data [1], approximately 1% of the global population, i.e., approximately 50 million people, suffer from epilepsy, and in China, the prevalence of epilepsy could reach 7.0‰, with approximately 9 million epilepsy patients. Despite the development of numerous antiepileptic drugs, only approximately 2/3 of patients' seizures can be effectively controlled, with 8%-10% of patients requiring surgery or neuromodulator techniques for treatment. In electrode implantation surgery, the electrodes implanted in the patient's skull are connected to the air, which could increase the risk of infection, bleeding, or even neurological damage [2]. Therefore, accurate techniques for the localization of the epileptogenic zone (EZ) are necessary to reduce the number of implanted intracranial electrodes and decrease the rate of infection. Otherwise, poor localization or incomplete signal acquisition could lead to secondary surgery and harm to the patient [3].

A promising diagnostic solution is to obtain internal information from the scalp via electromagnetic radiation, which can be used to locate abnormal sources in the cerebral cortex using the local or global source imaging of the measured electromagnetic signals. Electrophysiological source imaging (ESI) [4] is an inverse problem that aims to estimate the underlying activity of the brain using electroencephalography (EEG) data recorded from the

Manuscript received February 4, 2023; revised February 19, 2023; accepted February 27, 2023. Date of publication March 31, 2023; date of current version March 3, 2023.
* Corresponding Author, E-mail: gzxu@hebut.edu.cn
* Supported by the National Key R&D Program of China (2022YFC2402203) and the Key R&D Program of Hebei (21372002D).
Digital Object Identifier: 10.23919/CJEE.2023.000012

scalp. Based on mathematical models, ESI estimates the localization of scalp-recorded potentials and plots the sources of cerebral activity in a realistic head mode [5]. The development of ESI has provided more intriguing alternatives for locating the EZ from scalp EEG in the preoperative assessment of epilepsy [6].

Previous studies have attempted to localize the EZ based merely on the ESI of distributed inverse solution (DIS) methods with varying results [7]. However, the equivalent current dipole (ECD) method aims to define the location and/or orientation of single dipoles that best explain the EEG signal. Regarding the concept of network disorder, more sophisticated approaches may be required to identify the EZ from scalp EEG recordings accurately. During the interictal period, several brain regions participate in the epileptic network, and the challenge is to isolate the main driver of the network from the secondarily activated regions rather than finding the sources with the highest energy [8]. Functional brain connectivity analysis can be used to analyze the relationship between the sources calculated by ESI and may thus provide a more reliable EZ localization [9]. In this study, a previously published method that combines ESI and functional connectivity based on Granger causality is adapted. In the reported studies, the focus was merely on evaluating different families of “functional” connectivity methods, and the adapted version of the algorithm enables the successful analysis of directionality. We validated the approach using clinical scalp interictal EEG recordings from eight patients who were rendered seizure-free after surgery. The workflow is illustrated in Fig. 1.

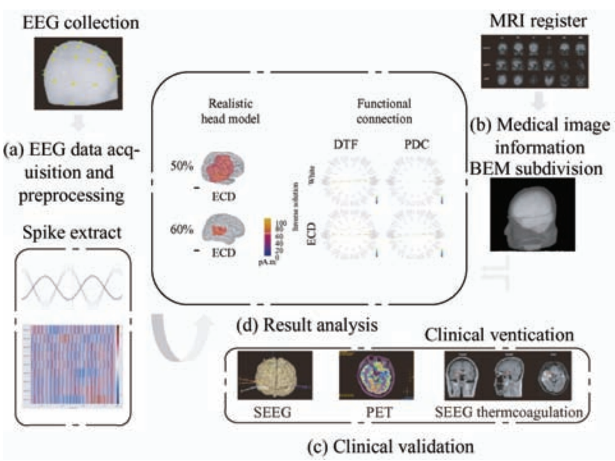

Fig. 1 Conceptual diagram of data analysis

2 Materials and methods

2.1 Subjects

Sixteen subjects, namely, eight epileptic patients and eight age- and sex-matched normal controls, participated in this study. The data of patients who underwent successful interictal epileptiform discharges (IEDs) were collected from Tianjin Huanhu Hospital. This study was approved by the Medical Ethics Committee of Hebei University of Technology. The demographic information of the patients and normal controls is shown in Tab. 1. All the participants provided written informed consent. Diagnostic imaging was performed by a certified radiologist and neurosurgeon according to the diagnostic protocols of the International League Against Epilepsy (ILAE) [10] and clinical signs (e.g., seizure presentation and exclusion zones).

Tab. 1 Demographics of patients and controls

Range of age	Number	Patients	Controls
10-20	3	16.7±1.527 5	17.8±1.235 6
20-30	2	27±2.828 4	24±1.414 2
30-40	2	37±2.828 4	35.5±4.949 7
50-60	1	55	48
Total	8	29.1±13.6	29.75±7.3

2.2 Noninvasive detection

With the development of image processing technology, research on the localization of the EZ using signal processing has gradually developed [11]. Scalp EEG, a noninvasive technology, routinely records the millisecond electrophysiological activity of neurons in patients and controls with strong global spatial coverage. According to the findings of several recent investigations, patients show significant abnormal patterns in scalp EEG during the interictal period. Therefore, scalp EEG is often considered a superior diagnostic tool for epilepsy compared with other electrophysiological methods. The operability of scalp EEG plays an irreplaceable role in the diagnosis of epilepsy, the early warning of seizures, and the localization of the EZ. Therefore, we could further guide the placement of intracranial electrodes by localizing the EZ in advance using noninvasive techniques.

2.3 EEG acquisition and preprocessing

EEG signals were collected prior to EZ removal surgery. Patients and controls underwent low-density scalp EEG recording (32 electrodes, Electrical Geodesics system) in accordance with the standard 10-20 system, with the data stored in European Data Format (EDF), at rest with eyes closed and were instructed to remain awake.

EEG is often contaminated by various physiological or nonphysiological sources of activity, such as cardiac signals, eye movements, and blinks [12] (Fig. 2a). Removing these artifacts using independent component analysis is a crucial step in producing noise-free signals prior to computing the EEG source (Fig. 2b). Owing to the high concentration of energy within the range of 0.5-80 Hz, the EEG signals were band-pass filtered in this band, restricting the frequency content of the signals to the ripple band of interest [13]. Furthermore, low frequencies could reduce baseline drift, and high frequencies could reduce muscle artifacts. A notch filter at 50 Hz was used to remove the industrial frequency interference (Fig. 2c).

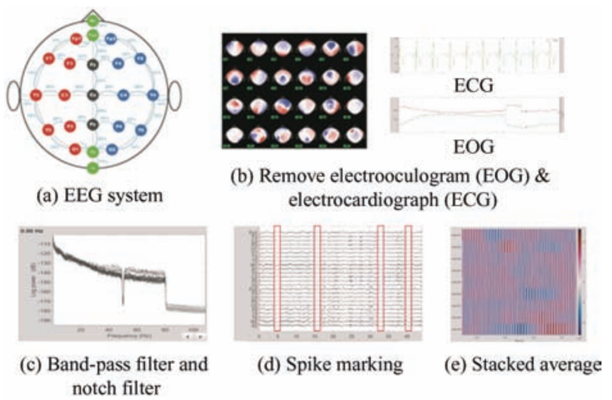

Fig. 2 Collection and preprocessing of EEG data

Over the last few decades, IEDs have emerged as biomarkers for the identification of epileptogenic tissue, which may improve the presurgical diagnosis and surgical outcome of patients with epilepsy. IEDs usually manifest as spikes (20-70 ms) and sharp waves (70-200 ms), with the spikes representing the synchronous release of excitatory postsynaptic potentials, which have emerged as potential presurgical biomarkers for the identification of the EZ. In this study, we visually selected portions of the EEG data with interictal activity occurring at least 2 h after clinical seizures. The EEG signals were manually labeled to identify the spikes, as shown in Fig. 2d. Then, the spikes were averaged to increase the signal-to-noise ratio further and used as input for ESI, as shown in Fig. 2e.

2.4 Forward model

ESI primarily addresses two major problems: the forward model and reverse localization. The forward model explains how signals generated by brain activity are transmitted to the scalp, and employs numerical calculations to describe the physical features of the brain [13-14]. The forward model is primarily intended to construct a model of the patients so that the physical structure and physical attributes of the head can be detailed in the analysis.

Researchers have sought to develop increasingly realistic models of the head using three-dimensional (3D) medical scanned images of heads. The boundary element method (BEM) [15] employs a given current source to calculate the conductor surface or boundary potential and requires only the discretization of the boundary. Using segmented magnetic resonance imaging (MRI) data, the source distribution was constrained to a field of current dipoles homogeneously distributed over the cortex and normal to the cortical surface. Therefore, the number of degrees of freedom of the boundary element can be reduced, resulting in a decrease in the spatial dimensionality of the solution.

The BEM [16] generally defines a three-layer model that accounts for the air/scalp, scalp/skull, and skull/brain interfaces. These contact surfaces must be very smooth and conductive, and each surface must be meshed into small triangular elements. The corresponding potential $v(r)$ at any point r on the uniform boundary element conductor is defined as follows

$$v(r)=\frac{2\sigma_0}{\sigma_k^- +\sigma_k^+}v_0(r)+\frac{1}{2\pi}\sum_{j=1}^{R}\frac{\sigma_j^- -\sigma_j^+}{\sigma_k^- +\sigma_k^+}\int_{r\in S_j} v(r')\frac{r'-r}{\left\|r'-r\right\|^3}\mathrm{d}S_j \tag{1}$$

where σ_0 corresponds to the medium, and $v_0(r)$ is the potential at point r. σ_j^- and σ_j^+ indicate the conductivities of the contact surface S_j internally and externally, respectively. dS is the vector of the orthogonal and contact surface elements. $\|\mathrm{d}S\|$ represents the contact surface element area. Each contact surface S_j was divided into N triangles. The potential of each triangle is calculated using the above equation. The potential of the contact surface S_j is defined as

$$v(r)=\frac{2\sigma_0}{\sigma_k^- + \sigma_k^+}v_0(r)+\frac{1}{2\pi}\sum_{k=1}^{R}\frac{\sigma_k^- - \sigma_k^+}{\sigma_k^- + \sigma_k^+}\sum_{j=1}^{N_{sk}}\int_{\Delta S_{kj}} v(r')\frac{r'-r}{\|r'-r\|^3}\mathrm{d}S_k \tag{2}$$

where R represents the number of contact surfaces within the conductor, and an exact integral is typically not possible.

2.5 Realistic head model

MRI methods can yield high imaging quality of the internal brain tissue, for which the spatial resolution could be 1 mm×1 mm or even smaller in terms of the intralayer pixel size and 2 mm to 1 mm or less in terms of the interlayer distance. In this study, we used the T1 MRI of epileptic patients to construct a realistic and subdivided head model.

(1) Read the MRI image: As the data read have no reference, it is necessary to set the reference point for the MRI image, including the left ear (LPA), right ear (RPA), nasion (NAS), anterior commissure (AC), posterior commissure (PC), and any interhemispheric point (IH), where NAS, LPA, and RPA are required to define the subject coordinate system and are used to register the EEG sensors on MRI. AC, PC, and IH are optional and are additional anatomical landmarks. The reference points are shown in Fig. 3.

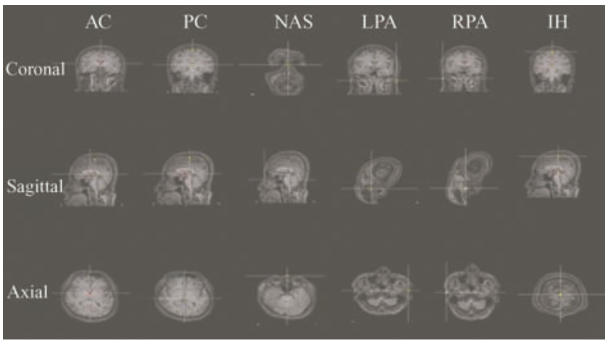

Fig. 3 MRI image reference points

(2) Segmentation: MRI imaging data were segmented to produce three layers: brain, skull, and scalp. To unify the coordinate space of all the images, the resulting images were linearly aligned to the standard template space of Montreal Neurological Institute (MNI), with a uniform separation of 10 mm, and labeled according to the automated anatomical labeling (AAL) atlas. Coordinate and affine transformations were performed on the images using the standard template.

(3) Meshing: A realistic head model was constructed based on the BEM for the segmented data, and triangles were used to represent the different tissues in the head model.

(4) Build a realistic head model using split and meshed data: Different conductivities must be specified for different head tissues. The conductivities of the scalp and brain tissue were both 1 and that of the skull was 0.012 5, and the number of vertices on each layer was 1 922. Each type of tissue was considered electrically homogenous and isotropic. The subdivisions and reconstructions of the realistic head model are shown in Fig. 4.

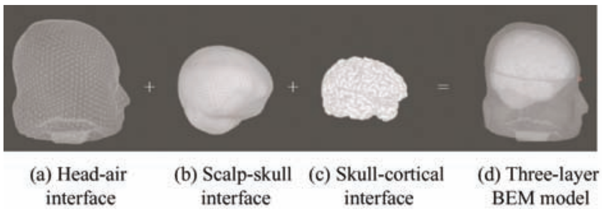

Fig. 4 Subdivision and reconstruction of the realistic head model

2.6 EEG source imaging

The inverse solution is mainly divided into two types: nonparametric and parametric methods [17]. Nonparametric methods are also referred to as DIS methods. The DIS divides the cortex surface into smaller voxels known as grids. Each active grid point indicates an active source, which makes the general problem underdetermined and ill-posed because the number of knowns (EEG signals from electrodes observed on the scalp) is much smaller than the number of source points [18]. The most popular methods include weighted maximum entropy on the mean (wMEM), standard low-resolution electromagnetic tomography (sLORETA) [19], dynamic statistical parametric mapping (dSPM), and weighted minimum norm estimate (wMNE) [20]. DIS can be expressed by the following equation

$$\boldsymbol{B} = \boldsymbol{L}S + \varepsilon \tag{3}$$

where $\boldsymbol{B} = \left[b_1, \cdots, b_n, \cdots, b_{n_c}\right]^{\mathrm{T}} \in R^{n_c \times \mathrm{T}}$ represents the signal flow of electrode n on the surface of the scalp over time period T, and n_c represents the number of surface electrodes. S represents the signal of the source, and $\boldsymbol{L} = \begin{pmatrix} l_{11} & \cdots & l_{1n_s} \\ \vdots & & \vdots \\ l_{n_c 1} & \cdots & l_{n_c n_s} \end{pmatrix}$ is the lead matrix of the function. Each element in the equation

$$L_{mn} = \left[l_{mnx}, l_{mny}, l_{mny}\right] \quad m = 1, \cdots, n_c; n = 1, \cdots, n_s \tag{4}$$

represents the contribution of the nth dipole source to the mth surface electrode, and the contribution of the dipole source inside the entire head model to the mth electrode can be expressed as follows

$$b_m = \sum_{n=1}^{n_s} b_{mn} = \sum_{n=1}^{n_s} l_{mn} S_n = \sum_{n=1}^{n_s} \left(l_{mnx} S_{nx} + l_{mny} S_{ny} + l_{mnz} S_{nz} \right) \tag{5}$$

Parametric methods are also referred to as ECD methods, or concentrated source or spatial-temporal dipole fit models [21]. These models range in complexity from a single dipole in a spherical head model to multiple dipoles (up to 10 or more) in a realistic head model. The ECD methods localize the EZ by processing and reconstructing the EEG using the electric field theory, mathematical principles, and computer technology. These models could correctly invert the position and direction of cerebral dipoles in three axes and the 3D spatial distance between localization spots, which might be accurate to the centimeter level. The ultimate output of most ECD methods is highly reliant on the initial approximation of the number of dipoles to be estimated [22], and their starting positions and orientations. In the optimal dipole, any point inside the sphere has an associated optimal dipole with the best dipole position and orientation, which fits the observed data better than any other dipole with the same location but different orientations [23].

2.7 Functional connectivity

The connectivity method at the level of the brain sources (source space) combines the excellent resolution of EEG with superior to exceptional spatial resolution [24]. The localization accuracy depends on the granularity (coarse to fine grain) of the source model used to solve the EEG inverse problem and identify networks at the cortical level. In epilepsy, Granger causality, a statistical concept of causality based on how well one signal can predict another, has frequently been used to localize the EZ from interictal ESI [25]. These promising results suggest that combining ESI and Granger causality may become an important alternative for localizing the EZ, aiding presurgical planning in patients with epilepsy [26].

3 Results and analysis

3.1 Validation against SEEG gold standard

For the proposed noninvasive interictal ESI, the final challenge is to find a validation strategy to quantify the performance of the method optimally. Stereoelectroencephalogram (SEEG) analyzes the location of the EZ by implanting electrodes on the brain, which is considered the gold standard for the clinical positioning of the EZ [27]. The evaluation of the surgical results is compared with the gold standard of SEEG in Fig. 5.

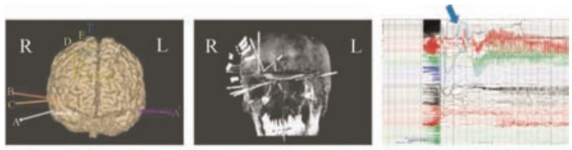

(a) Location of the implantation electrodes (b) Post-implantation CT of 3D orthogonal slices (c) iEEG of seizure period

Fig. 5 Validation of the SEEG gold standard (R: Right; L: Left)

Fig. 5a shows a 3D model of the patient's cerebral cortex after electrode implantation. The location of the implanted electrodes is shown in Fig. 5b. After the detection of SEEG electrodes, the spikes at the beginning of the seizure were detected by electrode point A2, which determined that the abnormal discharge was located in the amygdala and hippocampus region of the right temporal leaf of the brain.

3.2 Localization results

As evident from the plots in Fig. 6, a very high threshold, such as 70%, would lead to the loss of important information in the estimate. Additionally, lower thresholds cause the solution to be insufficiently accurate. However, the ECD method has an excellent coupling performance for focal neurological diseases. The DIS method analyzes focal neurological diseases without significant features in the energy distribution of the cerebral cortex in the localization results, and a relatively loose distribution is presented. From a comparison between Fig. 6 and the gold standard, it can be observed that the ECD method fits best when the threshold is 50%.

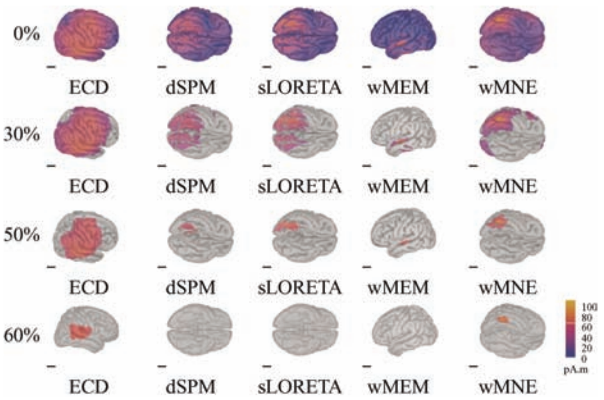

Fig. 6 Current density distribution result calculated from 5 ESI methods based on the realistic head model (The subscript under each model illustrates the threshold in percentage)

(1) The source imaging obtained based on the ECD method showed that the value with a relatively high current density distribution was located at the front of the temporal lobe. The source location was distributed near the amygdala by increasing the threshold of 50%. When the threshold value increased to 60%, some information was lost. Combining medical imaging and intracranial electroencephalography (iEEG), the EZ was comprehensively judged to be the amygdala with a threshold of 50%, which is consistent with the results obtained by iEEG.

(2) The dSPM, sLORETA, and wMNE are all accurate in terms of lateralization and are located on the right side of the brain. When the threshold value was below 50%, the source distribution was scattered and did not exhibit a good fit. When the threshold value was greater than 50%, important information was lost. Among the three DIS methods, the wMNE was closer to the true source.

(3) The source location obtained based on the wMEM could not refer to the location of the EZ, which is mainly located near the right middle temporal gyrus. The fixed side is not accurate, mainly because the wMEM is used to locate oscillatory activities [28].

3.3 Functional connectivity

The preferred techniques based on Granger causality for extracting interictal connectivity patterns are partial directed coherence (PDC) and directed transfer function (DTF) [29]. PDC models only direct connections, whereas DTF considers indirect and cascade connections [30]. The above localizion results show that the wMNE and ECD have significants. We performed a joint comparison of the above two inverse algorithms and Granger causality (PDC and DTF) and observed excellent matching. We used the Desikan-Killiany atlas to divide the regions of interest in the brain functional network.

The results obtained from Granger causality are shown in Fig. 7. Fig. 7a depicts the flow of information recorded intracranially, with identified spikes spreading from the A, B, C, and D to F electrodes, indicating that the abnormal discharge spreads from the right temporal to the right anterior lobe and insula. When combining ECD and DTF on the same scalp EEG data, the source connectivity approach retrieved a five-node network in the left temporal and right temporal regions, involving the fusiform, parahippocampal, entorhinal, and middle temporal regions. Compared with the normal causality network from the healthy controls (Fig. 7b), there are four abnormal information flows in the five nodes. The information alternated abnormally between hemispheres in the epileptic brain. The information flow from the entorhinal to the middle temporal region was consistent with the intracranial recordings. Compared with ECD/PDC, wMNE/ECD, and wMNE/DTF, the results were concordant with the intracerebral recordings in iEEG signals. ECD/DTF were identified by visual analysis as regions involved in the main interictal activity (entorhinal), and in the propagated interictal activity (middle temporal). These results might be explained by the better fit demonstrated by the accuracy of ECD localization.

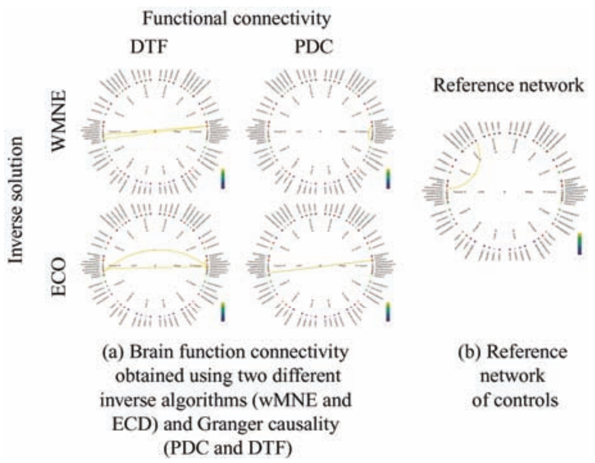

Fig. 7 Results of epilepsy patients and healthy controls obtained from Granger causality network

3.4 Quantitative analysis

SPSS 17.0 statistical software was used for data analysis, and count data are represented by [*n*(%)]. Tab. 2 shows a comparison of the results of various ESI methods and the gold standard.

Tab. 2 Comparison of ESI results and gold standard

Inverse algorithm	Match number of electrodes	Coincidence rate (*n*%)	χ^2	*p*
sLORETA (*n*=102)	93	91.18	7.439	0.006
wMEM (*n*=102)	90	88.24	10.714	0.001
wMNE (*n*=102)	96	97.06	4.293	0.035
dSPM (*n*=102)	92	90.20	8.518	0.004
ECD (*n*=102)	100	99.02	0.505	0.047

In this study, eight patients were implanted with a total of 102 electrodes: 48 on the left side and 54 on the right side. As a large sample of data is required for more accurate results in statistical analysis, we used the total number of electrodes implanted in all the patients as the sample size for data analysis. We used the Yates continuous calibration test to check the coincidence rate of various ESI methods and implanted electrodes, and $p<0.05$ was considered statistically significant for differences. The methods except the wMEM used in this study were accurate in the lateralization of the EZ, but the dSPM and sLORETA had some discrepancies with the electrode implantation location. The wMNE and ECD methods with a threshold of 50% were consistent with the gold standard in terms of lateralization and localization, which could provide a valid clinical reference. Compared with the localization of the gold standard, the difference was statistically significant ($p<0.05$). However, the localization range was less clinically significant based on the wMNE. From the quantitative analysis, the ECD method is more accurate in terms of lateralization and localization than the wMNE and has an excellent localization range.

According to the results, there are two hypotheses. ① The head model used in this study was computed using the BEM method with three layers (skin, skull, and brain). We developed a head model based on the BEM, where each volume element represents a dipole that focuses on the surface and may obtained a more accurate localization result combined with ECD method. Nevertheless, other methods exist for computing head models, such as the finite element method, or adding other layers, such as the cerebrospinal fluid [29]. These methods may affect the localization of the EZ. ② Another hypothesis is that the patients in this experiment had focal epilepsy. Focal epilepsy is typically caused by a focal point in the cerebral cortex. The DIS produces a diffusion effect for focal source localization, whereas the ECD produces a better fitting effect for the EZ. If epilepsy is generalized or the epileptic focus involves multiple regions of the brain, DIS can better represent multiple sources simultaneously.

4 Discussions

Scalp EEG is a noninvasive method that can collect spontaneous rhythmic electrophysiological activity in neurons. However, it is difficult to localize the EZ from the EEG owing to volume conduction and the frequent occurrence of artifacts during the interictal period. These challenges may be overcome by using a combination of ESI and functional connectivity analysis for low-density EEG recordings.

In 2014, Ted [31] tested different inverse solutions on ESI, which were lateralized in 47% of patients using the ECD method (75% accuracy) and in 29% of patients using the DIS method (60%-80% accuracy). Recently, Kovac et al. [32] used ESI based on ECD and DIS to localize the EZ in 87 patients. The results showed that using the ECD method yielded meaningful results in 79 cases, significantly more than the use of DIS (*n*=69). Nevertheless, these studies were unable to detect statistically significant and meaningful differences in the performance of various inverse models. We speculate that the ECD model usually represents the focal electrical activity. However, DIS models are more suitable for characterizing the extended sources.

Regarding the combination of the inverse solution algorithm and functional connectivity, most reported studies have empirically selected a combination that was shown to have a dramatic impact on the results, in terms of the identified network topology. Recently, Hassan et al. [33] in 2018 have used two DIS methods and two connectivity measures (phase locking value (PLV) and cross-correlation coefficient) for localization. The results showed that the method based on PLV combined with the wMNE inverse algorithm performed better. Moreover, this study focused on evaluating different connectivity methods regardless of the directionality of these connections. Two-directional connectivity algorithms were evaluated in this study. We focused on the method of causal connectivity of brain regions, which is an interesting supplementary feature in the context of EZ localization. Globally, the results revealed that the appropriate combination of inverse solution algorithms and connectivity measures could have a significant impact on EZ localization from scalp EEG signals. As each of the reverse and functional methods has its own assumptions and characteristics, there is no consensus yet regarding the best combination. Therefore, a deeper analysis of the combination of inverse algorithms and connectivity is required in the future.

5 Conclusions

Interictal ESI is a promising neurophysiological tool for the EZ localization in drug-resistant focal epilepsy. Connectivity analysis has been shown to add substantial information to pure ESI. According to the experimental results, the ECD method based on the realistic head model could obtain an accurate localization, and an appropriate combination of inverse algorithm and functional connectivity also helped substantially increase the interpretability and credibility of the result, which could provide a more valuable and objective interpretation of the scalp EEG. Clinically, the proposed method can guide the placement of intracranial EEG electrodes to reduce the number of intracranial electrodes, economic cost, and patient pain.

References

[1] X Shi, Z Zhang, Z Zhang, et al. Near-infrared window II fluorescence image-guided surgery of high-grade gliomas prolongs the progression-free survival of patients. *IEEE T. Bio-med. Eng.*, 2021, 69(6): 1889-1900.

[2] H Wu, Z He, X Zhang. Research progress on the role of inflammatory factors in epilepsy. *Military Medicine*, 2018, 42(10): 796-800.

[3] M Zijlmans, W Zweiphenning, N van Klink. Changing concepts in presurgical assessment for epilepsy surgery. *Nat. Rev. Neurol.*, 2019, 15: 594-606.

[4] S Kameyama, H Shirozu, H Masuda, et al. MRI-guided stereotactic radiofrequency thermocoagulation for 100 hypothalamic hamartomas. *J. Neurosurg*, 2016, 124: 1503-1512.

[5] M Zhu. The clinical application of CT in the diagnosis of epilepsy and its effect analysis. *Application of Modern Medicine in China*, 2015, 8: 38.

[6] W Staljanssens. Seizure onset zone localization from clinical ictal EEG in refractory epilepsy. *2017 Annual Meeting of the Organization for Human Brain Mapping*, 2017.

[7] L Astolfi, F Fallani, F Cincotti, et al. Estimation of effective and functional cortical connectivity from neuroelectric and hemodynamic recordings. *IEEE Transactions on Neural Systems and Rehabilitation Engineering*, 2008, 17(3): 224-233.

[8] L Lemieux, J Hand. Calculation of electrical potentials on the surface of a realistic head model by finite differences. *Physics in Medicine & Biology*, 1996, 41(7): 1079-1091.

[9] L Maillard, E Rikir, M Gavaret, et al. Electrical source imaging in cortical malformation-related epilepsy: A prospective EEG-SEEG concordance study. *Epilepsia*, 2014, 55: 918-932.

[10] D Pascual. Standardized low-resolution brain electromagnetic tomography(sLORETA): Technical details. *Methods and Fidings in Experimental and Clinical Pharmacology*, 2002, 24: 418-424.

[11] G Birot. Head model and electrical source imaging: A study of 38 epileptic patients. *Neuroimage Clin.,* 2014, 5:

77-83.

[12] A H H Seyed, S Abbas, A Mehmet, et al. Electromagnetic brain source imaging by means of a robust minimum variance beamformer. *IEEE T. Bio-med. Eng.*, 2018, 65(10): 2365-2374.

[13] P Megevand, L Spinelli, M Genetti, et al. Electric source imaging of interictal activity accurately localises the seizure onset zone. *J. Neurol. Neurosurg. Psych.,* 2014, 85(1): 38-43.

[14] R Andrea, P Cristina, F Alessandro, et al. A two-step inverse-scattering technique in variable-exponent lebesgue spaces for through-the-wall microwave imaging: Experimental results. *IEEE Trans. GRS*, 2021: 1-12.

[15] J W Meijs, O W Weier, M J Peters, et al. On the numerical accuracy of the boundary element method. *IEEE T. Bio-med. Eng.*, 1989, 36(10): 1038-1049.

[16] S Baillet, J C Mosher, R M Leahy. Electromagnetic brain mapping. *IEEE Signal Processing Magazine,* 2001, 18(6): 14-30.

[17] W Staljanssens, G Strobbe, R Van Holen, et al. EEG source connectivity to localize the seizure onset zone in patients with drug resistant epilepsy. *NeuroImage: Clinical*, 2017, 16: 689-698.

[18] B Kamousi, Z Liu, B He. Classification of motor imagery tasks for brain-computer interface applications by means of two equivalent dipoles analysis. *IEEE Transactionson Neural Systems and Rehabilitation Engineering*, 2005, 13(2): 166-171.

[19] L Guo, Y Wang, H Yu, et al. Brain functional network based on approximate entropy of EEG under magnetic stimulation at acupuncture point. *Transactions of China Electrotechnical Society*, 2015, 30(10): 31-38.

[20] M Sandhya, R D Bharath, R Panda, et al. Understanding the pathophysiology of reflex epilepsy using simultaneous EEG-fMRI. *Epileptic Disorders*, 2014, 16(1): 19-29.

[21] A Sohrabpour, S Ye, G A Worrell, et al. Noninvasive electromagnetic source imaging and Granger causality analysis: An electrophysiological connectome (eConnectome) approach. *IEEE Transactions on Biomedical Engineering*, 2016, 63(12): 2474-2487.

[22] D Chen, S Wan, F Bao. Epileptic focus localization using discrete wavelet transform based on interictal intracranial EEG. *IEEE T. Neur. Sys. Reh.*, 2017, 25(5): 413-425.

[23] M Stenroos, O Hauk. Minimum-norm cortical source estimation in layered head models is robust against skull conductivity error. *NeuroImage*, 2013, 81: 265-272.

[24] A M Dale, A K Liu, B R Fischl, et al. Dynamic statistical parametric mapping: Combining fMRI and MEG for high-resolution imaging of cortical activity. *Neuron*, 2000, 26(1): 55-67.

[25] J Bai, W Zhou, H Wang, et al. Value of stereoelectroencephalography (SEEG)-guided radiofrequency thermocoagulation in treating drug-resistant focal epilepsy. *Brain Science Advances*, 2019, 5(3): 53-66.

[26] K Kaiboriboon, H Lüders, M Hamaneh, et al. EEG source imaging in epilepsy-practicalities and pitfalls. *Nature Reviews Neurology*, 2012, 8(9): 498-507.

[27] A Coito, M Genetti, F Pittau, et al. Altered directed functional connectivity in temporal lobe epilepsy in the absence of interictal spikes: A high density EEG study. *Epilepsia*, 2016, 57(3): 402-411.

[28] P Van, M Papadopoulou, E Carrette, et al. Functional brain connectivity from EEG in epilepsy: Seizure prediction and epileptogenic focus localization. *Prog. Neurobiol.*, 2014, 121: 19-35.

[29] Z Cai, A Sohrabpour, H Jiang, et al. Noninvasive high-frequency oscillations riding spikes delineates epileptogenic sources. *Neuroscience*, 2021, 118(17): 1-12.

[30] S Liu, J Parvizi. Cognitive refractory state caused by spontaneous epileptic high frequency oscillations in the human brain. *Sci. Transl. Med.,* 2019, 11(514): 1-12.

[31] S Ted. A wide equivalent circuit electric dipoles. *IEEE T. Antenn. Propag.*, 2020, 68(11): 7636-7639.

[32] S Kovac, U J Chaudhary, R Rodionov, et al. Ictal EEG source imaging in frontal lobe epilepsy leads to improved lateralization compared with visual analysis. *J. Clin. Neurophysiol.*, 2014, 31(1): 10-20.

[33] M Hassan, I Merlet, A Mheich, et al. Identification of interictal epileptic networks from dense-EEG. *Brain Topography*, 2016, 30(1): 60-76.

Ruowei Qu received her B.S. degree from the School of Science, University of Science and Technology Beijing, Beijing, China in 2012. She finished her Ph.D. in Electrical Engineering from Hebei University of Technology, Tianjin, China in 2020 and currently working as a Post Doctor at this university. During the year of 2015 to 2016, she was a Visiting Scholar at Department of Computational Neurology in University of Pittsburg, USA. She is currently working on the epilepsy zone localization problem based on multi-model medical data.

Zhaonan Wang received her B.S. degree at Shandong University of Traditional Chinese Medicine in 2017. She is currently pursuing a master degree in Hebei University of Technology, Tianjin, China. Her research interests include epilepsy zone localization and electrophysiological source imaging.

Shifeng Wang received his B.S. degree in Medicine from Tianjin Medical University in 2007. He is currently studying for a master degree at the Department of Nuclear Medicine, Cancer hospital of Tianjin Medical University, Tianjin, China. His research interests include multimodal imaging evaluation of epilepsy and PET imaging of systemic tumor.

Le Wang received his B.S. degree from the School of Medicine, Hebei North University, Zhangjiakou, China, in 2008 and received his M.S. in Oncology from Tianjin Medical University, Tianjin, China, in 2011. He finished his M.D. in Surgery from Tianjin Medical University, Tianjin, China, in 2022 and currently working as a Doctor-in-Charge at neurosurgery of Tianjin Huanhu Hospital, Tianjin, China. He is currently working on the epilepsy zone localization problem and epileptic networks based on multimodal medical data.

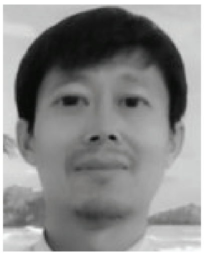

Alan Wang is a Principal Investigator and Associate Professor at Auckland University. He has more than ten years of research experience in bioengineering informatics and integrated medicine, especially in advancing the role of medical informatics in health care. His research interests include bioengineering, data informatics, neurocomputing, and biomedical statistics and simulation. He has developed medical data analytics methods for mobile health and personalized diagnosis and prognosis based on intelligent computing theories. He has experience analyzing huge cohorts of patient data with applications of early diagnosis, disease understanding, and effective treatment of patients with different disorders. He serves as an Editorial Board Member and an Active Reviewer for several international journals.

Guizhi Xu was born in 1962. She received a Ph.D. degree from the School of Electrical Engineering, Hebei University of Technology, Tianjin, China in 2002. She is currently a Professor, Doctoral Advisor and the Dean of School of Electrical Engineering, Hebei University of Technology, Tianjin, China. She is also the Head of Key Subjects at the Provincial Level of Biomedical Engineering, a Professor of Meta-optics of Hebei University of Technology, and the Head of the National Top-quality Course of Engineering Electromagnetic Field.

She published more than 90 academic papers retrieved by SCI and Ei, and published 3 monographs. She presided over 1 key project of the National Natural Science Foundation, 3 projects of the National Natural Science Foundation and one pre-research project of the Ministry of General Equipment, and completed 2 key projects of the National Natural Science Foundation in cooperation with Tsinghua University and the Fourth Military Medical University. She achieved Hebei Science and Technology Outstanding Contribution Award 1, Hebei Natural Science Second Prize and Third Prize 1, Hebei Science and Technology Progress Second Prize and Third Prize 1, and Hebei Excellent Teaching Achievement Second Prize 3.

She achieved the honorary titles of the First Famous Teaching Teacher in Hebei Province, the Outstanding Young and Middle-Aged Experts in Hebei Province, the Outstanding Young and Middle-Aged Backbone Teachers in Hebei Province, the Advanced Individuals in Hebei Province, and the Outstanding Communist Party Members in Hebei Province’s education system.